

Grasp the Graph (GtG) 2.0: Ensemble of GNNs for High-Precision Grasp Pose Detection in Clutter

Ali Rashidi Moghadam^{1*}, Sayedmohammadreza Rastegari^{2*}, Mehdi Tale Masouleh¹, Ahmad Kalhor¹
Human and Robot Interaction Laboratory, School of Electrical and Computer Engineering,
University of Tehran, Tehran, Iran

¹{ali.rashidi.m, m.t.masouleh, akalhor}@ut.ac.ir, ²s.mohammadreza.rastegari@gmail.com

Abstract—Grasp pose detection in cluttered, real-world environments remains a significant challenge due to noisy and incomplete sensory data combined with complex object geometries. This paper introduces *Grasp the Graph 2.0 (GtG 2.0)* method, a lightweight yet highly effective hypothesis-and-test robotics grasping framework which leverages an ensemble of Graph Neural Networks for efficient geometric reasoning from point cloud data. Building on the success of GtG 1.0, which demonstrated the potential of Graph Neural Networks for grasp detection but was limited by assumptions of complete, noise-free point clouds and 4-Dof grasping, GtG 2.0 employs a conventional Grasp Pose Generator to efficiently produce 7-Dof grasp candidates. Candidates are assessed with an ensemble Graph Neural Network model which includes points within the gripper jaws (*inside points*) and surrounding contextual points (*outside points*). This improved representation boosts grasp detection performance over previous methods using the same generator. GtG 2.0 shows up to a 35% improvement in Average Precision on the GraspNet-1Billion benchmark compared to hypothesis-and-test and Graph Neural Network-based methods, ranking it among the top three frameworks. Experiments with a 3-Dof Delta Parallel robot and Kinect-v1 camera show a success rate of 91% and a clutter completion rate of 100%, demonstrating its flexibility and reliability.¹

Index Terms—Grasp Pose Detection, Grasping in Clutter, Graph Neural Networks, Ensemble Learning

I. INTRODUCTION

Robotic grasping is a fundamental capability which enables robots to interact with the physical world, with applications ranging from industrial automation to domestic assistance. Although this skill comes naturally to humans, it has remained a significant challenge in robotics due to the complexity of object geometries, textures, and the inherent noise and incompleteness of sensor data. Traditional methods typically evaluate grasp poses by focusing on the geometric relationship between the gripper and the object—a strategy that underpins many analytical metrics for grasp quality. In this context, Graph Neural Networks (GNNs) [1], [2] have emerged as an intriguing tool for geometric learning, offering an inductive bias which facilitates more efficient learning of these spatial relationships compared to conventional neural network architectures.

*Equal Contribution.

¹Related codes will be available at <https://github.com/Ali-Rashidi/GtG2>

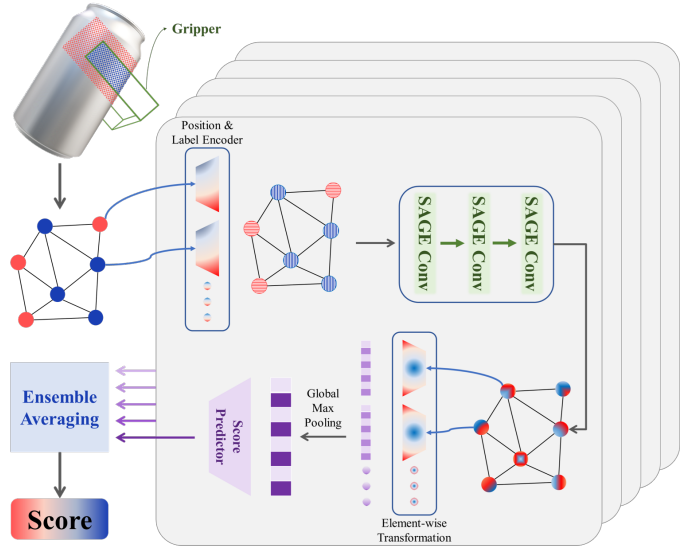


Fig. 1. Overview of the ensemble GNN architecture. At each gripper pose, two sets of points are sampled: *inside points* (blue) and *outside points* (red). A local graph is constructed by connecting these points via KNN. Each input graph (with *blue nodes* and *red nodes*) is processed by an ensemble of five GNN-based regressors sharing the same architecture but trained with different weights. Each regressor produces a grasp score, and the final score is the average of these five outputs. The pipeline comprises a Position & Label Encoder, a stack of SAGEConv layers, an element-wise transformation, global max pooling, and an MLP score predictor.

Despite the advances brought by deep learning, many models incur substantial computational costs that may not be suitable for applications on resource-constrained systems. In previous work, the *Grasp the Graph (GtG) 1.0* [3] framework was introduced as a novel approach to represent point clouds as graphs for robotic grasp detection using GNNs. The name *GtG* reflects the strategy of leveraging graph representations to capture the geometric relationships between the gripper and objects. GtG 1.0 [3] demonstrated the potential of GNNs in grasp detection; however, it was constrained by several critical limitations. First, it relied on assumptions of complete, noise-free point clouds, which are rarely encountered in real-world scenarios. Second, it employed uniform random sampling for 4-Dof grasp generation, a strategy which is inefficient and impractical for crowded scenes and higher-Dof grasping. Third, it processed the entire scene graph to predict the success prob-

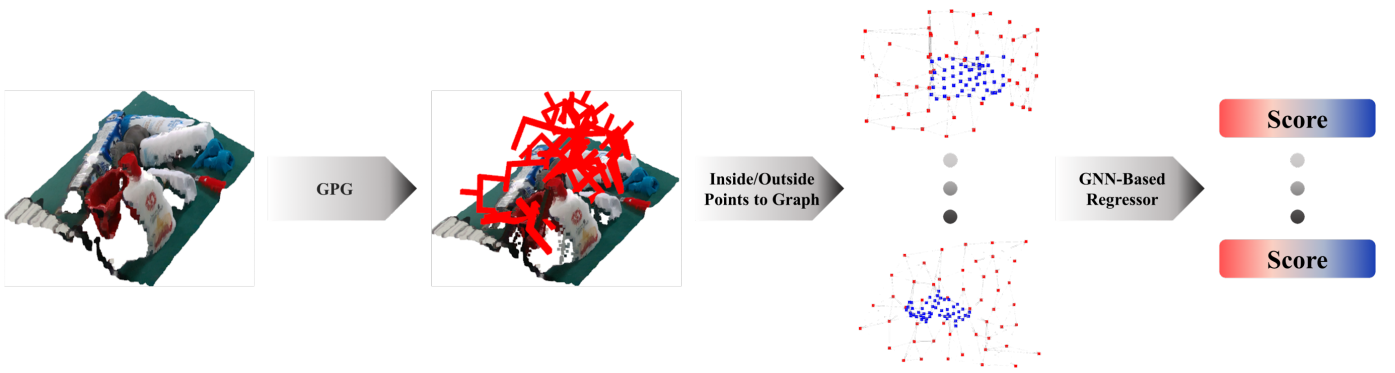


Fig. 2. Illustration of the GtG 2.0 pipeline. A cluttered point cloud is processed by the Grasp Pose Generator (GPG) to propose candidate grasps. A sample of each candidate’s **inside points** and **outside points**, sampled using furthest point sampling (FPS), forms a local graph using KNN, which is then fed into an ensemble of GNN-based regressors for final grasp scoring.

ability of a single grasp pose, despite the fact that objects far from the grasp candidate are often irrelevant to grasp success. This approach not only increases computational complexity but also makes it challenging to learn a meaningful correspondence between an arbitrary grasp pose and the scene graph, particularly in cluttered environments. In this paper, **Grasp the Graph 2.0 (GtG 2.0)** is introduced as a significantly enhanced hypothesis-and-test framework that addresses these limitations. The proposed framework begins by employing the Grasp Pose Generator (GPG) [4], a heuristic algorithm developed to extract 7-Dof grasp poses for a parallel-jaw gripper directly from raw point cloud data, to efficiently generate diverse grasp candidates, thereby overcoming the inefficiencies of exhaustive or random sampling. The grasp candidates are subsequently evaluated by an ensemble of lightweight GNN models which process graphs representing both “inside points” (within the gripper jaws) and “outside points” (surrounding the grasp region). This enriched geometric context allows the unobserved areas of objects in point clouds to be reasoned about, thereby enabling robust detection of grasp poses even in cluttered and occluded environments. The ensemble GNN approach leverages multiple independently trained networks with similar architectures to reduce overfitting and improve generalization. Performance improvements of up to 35% in Average Precision (AP) have been achieved over conventional hypothesis-and-test and GNN-based methods, placing GtG 2.0 among the top methods for grasp pose detection, while the proposed method requires significantly fewer parameters. In addition, real-world experiments conducted on a 3-Dof Delta Parallel robot equipped with a two-finger gripper, which enables 4-Dof grasping, and a Kinect-v1 sensor, demonstrate a 91% grasp success rate and a 100% task completion rate across various cluttered scenarios. These results not only demonstrate the superior performance of GtG 2.0 but also highlight its potential for real-world deployment in various settings, considering its flexible and reliable pipeline. In summary, the contributions of this paper are:

- **A novel GNN framework** which combines efficient candidate generation with lightweight, context-rich grasp evaluation, significantly reducing computational complexity while enhancing robustness using an ensemble of

models in cluttered environments.

- **A context-rich grasp representation** that integrates both inside and outside points, enabling robust detection of grasp poses even in partially observed and occluded environments.
- **Extensive experimental validation** that demonstrates the effectiveness and generalizability of the proposed method on benchmark datasets and real-world robotic systems, achieving a 91% grasp success rate and a 100% task completion rate across diverse cluttered scenarios.

The remainder of the paper is organized as follows. In Section II, a comprehensive review of the current state-of-the-art in robotic grasping is provided, with both conventional methods and recent advances, including ones employing GNNs. In Section III, the proposed approach is described in detail, and the design and implementation of the GtG 2.0 framework are presented—from the grasp candidate generation and graph representation construction to the ensemble GNN-based scoring mechanism and training strategies. In Section IV, an extensive evaluation of the method is presented, including benchmark comparisons, ablation studies, and real-world experiments that demonstrate the robustness and precision of the framework. Finally, in Section V, the key findings are summarized, the implications of the research are discussed, and promising directions for future work in grasp detection and manipulation in cluttered environments are outlined.

II. RELATED WORK

Advances in data-driven grasp pose detection have led to a variety of methods, which can be broadly categorized into *Hypothesize-and-Test* and *End-to-End* approaches [5]. These paradigms differ in their approach to candidate generation and evaluation, with each offering unique advantages and challenges. The following sections summarize these approaches before discussing recent developments using GNNs in grasp detection.

A. Hypothesize-and-Test Grasp Pose Detection

In Hypothesize-and-Test methods, the grasp detection problem is divided into two stages: candidate generation and candidate evaluation. A candidate generator produces potential

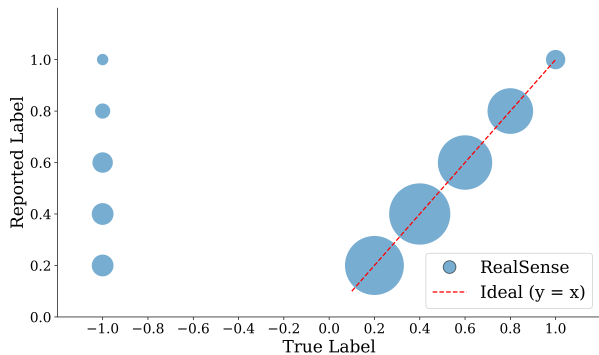


Fig. 3. Illustration of label discrepancies in GraspNet: the horizontal axis shows original GraspNet-1Billion scores, while the vertical axis represents recalculated quality. Many grasps labeled “valid” by GraspNet (upper right region) are deemed collision-prone or infeasible upon reevaluation.

grasp poses using different heuristics, which are then assessed by a separate model. This modular design offers flexibility, as the generator and evaluator can be optimized independently for specific tasks or sensor configurations. For example, GQ-CNN [6] is trained on a large synthetic dataset where each depth image is paired with a parallel-jaw grasp specification and an analytic robustness metric derived from physics-based models. At inference, the model quickly predicts the success probability of each candidate, facilitating efficient ranking and selection. Similarly, GPD [7] employs GPG to sample candidates, followed by a CNN-based classifier. While these methods have shown promise, they often struggle with the computational cost of processing large numbers of candidates and the challenge of generalizing to unseen objects and environments. Improvements in handling raw point cloud data have also been explored. PointNet [8] preserves the permutation invariance of point clouds and processes them more effectively than voxel or grid-based methods. Building on this, PointNetGPD [9] and 3DSGrasp [10] further refine grasp detection; the latter, for instance, enhances accuracy by first completing missing parts of the point cloud. These methods demonstrate the potential of directly processing point clouds, but they often require large datasets and computational resources, limiting their applicability in real-time scenarios.

B. End-to-End Grasp Pose Detection

End-to-End methods integrate candidate generation and evaluation within a single unified network. These approaches exploit local or global scene features to directly propose high-quality grasp candidates and assess them without the need for a separate classification stage. This integration often leads to more efficient and cohesive systems, but it can also increase the complexity of training and inference. For instance, RGB Matters [11] predicts gripper views and analytically computes grasp parameters such as width and depth. REGNet [12] employs a three-stage network comprising a Score Network (SN) for grasp confidence regression, a Grasp Region Network (GRN) for proposal generation, and a Refine Network (RN) for further enhancement of proposal accuracy. These methods demonstrate the potential of end-to-end learning but

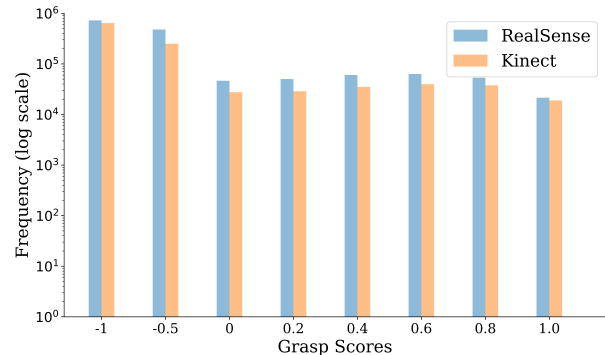


Fig. 4. Histogram of grasp scores from RealSense and Kinect cameras.

often require large amounts of labeled data and computational resources. Other approaches, such as GSNet [13] and HGGD [14], utilize geometric cues and grasp heatmaps to guide detection. LF-GraspNet [15] integrates a conditional VAE conditioned on structured local TSDF features to jointly learn scene geometry encoding and grasp configuration generation. SCNet [16] is an end-to-end category-level object pose estimation network that directly learns to deform and refine shape priors for one-shot 6-DOF pose prediction. Furthermore, [17] presents a grasp detection method based on object decomposition, which leverages multi-modal input (RGB and RGB-D images) and focuses on primitive shape abstraction. More recent methods like FlexLoG [18] and RNGNet [19] propose unified representations and integrated guidance mechanisms that further boost grasp detection accuracy. While these methods have achieved impressive results, they often rely on complex architectures which may not be suitable for resource-constrained systems.

C. Graph Neural Networks in Grasp Pose Detection

GNNs have emerged as an effective tool for grasp detection by modeling the spatial and relational structure of point cloud data. In these methods, point clouds are represented as graphs in which nodes correspond to points or features and edges capture spatial relationships. This representation allows GNNs to efficiently reason about the geometric relationships between the gripper and objects, making them particularly well-suited for grasp detection in cluttered and dynamic environments. One approach [20] formulates cluttered scenes as graphs, where nodes represent object geometries and edges encode their spatial relationships, allowing a GNN to evaluate the graph and propose feasible 6-Dof grasps for target objects. Similarly, GraNet [21] constructs multi-level graphs at the scene, object, and grasp point levels, and employs a structure-aware attention mechanism to refine local relationships and improve grasp predictions. These methods demonstrate the potential of GNNs for grasp detection but often require complex architectures and large amounts of training data. Other studies have integrated GNNs with reinforcement learning to handle dynamic or deformable objects [22], dividing the task into pre-grasp and in-hand stages. The GtG 1.0 framework also leverages GNNs to process point clouds efficiently by framing grasping as a one-step reinforcement learning problem

TABLE I
RESULTS ON GRASPNET DATASET FOR HYPOTHESIS-AND-TEST
METHODS, SHOWING AVERAGE APs OF EACH SCENE TYPE ON
REALSENSE/KINECT SPLIT.

Method	Backbone	#Params	Average (APs(%))
GPD [4]	CNN	3.6M	17.48 / 19.05
PointNetGPD [9]	PointNet	1.6M	19.29 / 20.88
GtG2.0 (Ours)	GNN	0.57M	53.42 / 47.00

without requiring large, complex networks. Additionally, a dual-branch GNN-based method [23] uses one branch to learn global geometric features and another to focus on high-value grasping locations, further enhancing grasp detection performance. These approaches highlight the versatility of GNNs for grasp detection but also underscore the need for lightweight and efficient architectures that can operate on resource-constrained systems.

III. THE GTG 2.0 FRAMEWORK: DESIGN AND IMPLEMENTATION

This section outlines the architecture and workflow of the GtG 2.0 framework, which detects high-quality 7-Dof grasp poses in cluttered environments, along with implementation details and the training process. Section III-A introduces GPG, while Section III-B describes how candidate poses are encoded into a graph representation that includes both points within the gripper jaws and contextual points for enhanced spatial evaluation. In Section III-C, the lightweight GNN architecture is detailed, which predicts grasp quality scores. Sections III-D and III-E discuss the creation of a high-quality training dataset and the implementation process. This includes strategies for addressing class imbalance and optimizing performance, such as employing an ensemble approach to enhance robustness and accuracy. As illustrated in Figure 2 and detailed in Algorithm 1, our overall pipeline starts with raw sensor input and proceeds through a series of steps to propose grasp poses along with their associated quality scores. Specifically, GtG 2.0 first employs GPG to extract candidate grasps from the incoming point cloud, then applies workspace filtering and depth inpainting to improve candidate reliability. Next, a local graph representation is constructed for each candidate—by sampling both the points inside the gripper (inside points) and those in the surrounding area (outside points) using FPS [24] and k-nearest neighbors—to capture the relevant spatial and contextual details. Finally, an ensemble of lightweight GNNs processes these graphs to predict and aggregate grasp quality scores, delivering a robust and efficient grasp pose detection pipeline.

A. Grasp Pose Generator (GPG)

Candidate grasp generation is performed using GPG. The Python implementation from [25] is employed, with several modifications introduced to enhance the generation of valid grasps. By default, GPG removes outlier points that are distant from their neighbors. However, this removal often

Algorithm 1 Prediction Pipeline of GtG 2.0

- 1: **Input:** Raw point cloud data, Ensemble of trained models $\{M_1, M_2, \dots, M_5\}$
- 2: **Output:** Final grasp quality scores for each candidate grasp
- 3: **// Step 1: Candidate Generation from Raw Data**
- 4: $candidates \leftarrow GPG(\text{RawPointCloud})$
- 5: $candidates \leftarrow \text{FilterWorkspacePlane}(candidates)$
- 6: $candidates \leftarrow \text{DepthInpainting}(candidates)$
- 7: $candidates \leftarrow \text{NonMaxSuppression}(candidates, \Delta\text{Parallel}T, \Delta\text{Parallel}\alpha)$
- 8: **// Step 2: Graph Representation Construction for Each Candidate**
- 9: **for** each candidate in $candidates$ **do**
- 10: Extract *inside* and *outside* regions from the candidate
- 11: $inside \leftarrow \text{FPS}(candidate.insideRegion, \text{maxPoints} = 70)$
- 12: $outside \leftarrow \text{FPS}(candidate.outsideRegion, \text{maxPoints} = 70)$
- 13: $G \leftarrow \text{ConstructKNNGraph}(inside \cup outside, k = 5)$
- 14: Store G in CandidateGraphs
- 15: **end for**
- 16: **// Step 3: Ensemble Prediction for Grasp Quality**
- 17: **for** each candidate graph G in CandidateGraphs **do**
- 18: Initialize list: $scores \leftarrow []$
- 19: **for** each model M in $\{M_1, M_2, \dots, M_5\}$ **do**
- 20: $s \leftarrow M.Predict(G)$ *// Compute grasp score for G*
- 21: Append s to $scores$
- 22: **end for**
- 23: $G.final_score \leftarrow \text{Average}(scores)$
- 24: **end for**
- 25: **Return** CandidateGraphs with their final grasp quality scores

results in grasp candidates being positioned too close to the object surface, potentially leading to unintended collisions. To address this issue, the outlier-removal step has been disabled. Additionally, the algorithm tends to generate many grasp candidates along the workspace plane, most of which are not viable. A plane detection method is applied to identify the workspace plane, and candidates that engage with its edges are subsequently removed. Limited sensor coverage and occlusions can create missing or null regions in the point cloud, prompting GPG to propose grasps in unreliable areas. A depth-map inpainting filter is incorporated to fill these voids with averaged estimates. Although the inpainting process may introduce minor artifacts, it generally yields more conservative grasp proposals that are less prone to collisions. Finally, both the inpainted and original (non-inpainted) point clouds are processed by GPG, and Non-Maximum Suppression (NMS) is applied, with thresholds of $\Delta\text{Parallel}T = 5\text{mm}$ and $\Delta\text{Parallel}\alpha = 1^\circ$, to eliminate near-duplicate grasps.

TABLE II
COMPARISON OF THE GNN-BASED GRASP POSE DETECTION METHODS ON THE GRASPNET DATASET, SHOWING AVERAGE APs OF EACH SCENE TYPE ON REALSENSE/KINECT SPLIT.

Method	Category	Average (APs(%))
GraNet [21]	End-to-End	32.73 / 29.44
Zhuang, C. et al. [23]	End-to-End	36.99 / 32.88
GtG2.0 (Ours)	Hypothesis-and-Test	53.42 / 47.00

B. Graph Representation of Grasp Candidates

After generation, each grasp candidate is encoded as a graph in the gripper’s local coordinate frame. In contrast to prior approaches like GPD and PointNetGPD, which sample only points located strictly between the gripper jaws (termed *Inside Points*), additional points outside the grasp region (termed *Outside Points*) are also incorporated. The inclusion of Outside Points aids in collision detection and facilitates reasoning about the geometry of the null space based on the surrounding context. To effectively represent each grasp candidate, FPS is applied separately to both Inside and Outside regions, selecting up to 70 points from each. This procedure ensures preservation of critical spatial details without excessive computational complexity. Each selected point is represented by a 3-Dimensional feature vector $[x, y, z, \text{inside/outside}]$. Subsequently, a k -nearest neighbor ($k = 5$) graph is constructed. Node labels are intentionally disregarded during graph construction, enabling effective feature exchange and spatial reasoning between the Inside and Outside regions.

C. GNN-Based Grasp Pose Score Prediction

As illustrated in Figure 4, a substantial number of generated grasp candidates have negative scores, indicating either collisions (score = -1) or low grasp quality (score = -0.5). Consequently, predicting grasp quality is crucial. This task is formulated as a regression problem, assigning a score of -1.0 to collision grasps, -0.5 to low-quality grasps, and incremental scores from 0 to 1 in intervals of 0.2 for valid grasps, with higher values signifying better stability and alignment. To predict grasp scores, each node feature of the candidate graph is first encoded into a higher-dimensional representation via an encoding Multi-Layer Perceptron (MLP). Let $\mathbf{x}_i \in \mathbb{R}^{d_{in}}$ denote the initial feature vector of node i . The encoding MLP transforms \mathbf{x}_i through a sequence of linear mappings, batch normalizations, and ReLU activations:

$$\begin{aligned} \mathbf{z}_i^{(1)} &= \text{ReLU}\left(\text{BN}_1(\mathbf{W}_1 \mathbf{x}_i)\right), \\ \mathbf{z}_i^{(2)} &= \text{ReLU}\left(\text{BN}_2(\mathbf{W}_2 \mathbf{z}_i^{(1)})\right), \\ \mathbf{z}_i &= \text{BN}_3(\mathbf{W}_3 \mathbf{z}_i^{(2)}), \end{aligned}$$

where $\mathbf{W}_1 \in \mathbb{R}^{d_h \times d_{in}}$, $\mathbf{W}_2 \in \mathbb{R}^{2d_h \times d_h}$, $\mathbf{W}_3 \in \mathbb{R}^{d_h \times 2d_h}$ are learnable weight matrices, d_h is the hidden dimension, and BN_k denotes the k th batch normalization layer.

Subsequently, the graph undergoes three layers of graph convolution using the SAGEConv operator [26]. Formally, the SAGEConv operation is defined as:

$$\mathbf{h}'_i = \mathbf{W}_1^{\text{sage}} \mathbf{h}_i + \mathbf{W}_2^{\text{sage}} \cdot \text{Max}\left(\{\mathbf{h}_j : j \in \mathcal{N}(i)\}\right),$$

where \mathbf{h}_i and \mathbf{h}'_i denote the input and updated feature vectors of node i ; $\mathcal{N}(i)$ represents the set of neighbors of node i ; $\mathbf{W}_1^{\text{sage}}$ and $\mathbf{W}_2^{\text{sage}}$ are learnable weight matrices; and $\text{Max}(\cdot)$ computes the maximum of the features of the neighboring nodes. Following graph convolution, each final node embedding vector h_i is refined individually through an element-wise transformation:

$$h'_i = a(h_i) \cdot h_i + b(h_i),$$

where $a(h_i)$ and $b(h_i)$ are learned vectors representing the slope and bias applied element-wise to h_i . After refinement, a global max pooling operation aggregates all node embeddings into a single graph-level descriptor. This operation is expressed as:

$$\mathbf{h}_{\text{global}} = \max_{i \in \mathcal{V}} \{h'_i\},$$

where \mathcal{V} denotes the set of all nodes in the graph and the maximum is computed element-wise. Finally, the global descriptor is processed by a score predictor MLP to estimate the final grasp quality score. Let $\mathbf{h}_{\text{global}} \in \mathbb{R}^{d_h}$ be the pooled feature vector; the predictor MLP computes:

$$\begin{aligned} \mathbf{s}^{(1)} &= \text{ReLU}\left(\text{BN}'_1(\mathbf{W}'_1 \mathbf{h}_{\text{global}})\right), \\ \mathbf{s}^{(2)} &= \text{ReLU}\left(\text{BN}'_2(\mathbf{W}'_2 \mathbf{s}^{(1)})\right), \\ s &= \mathbf{W}'_3 \mathbf{s}^{(2)}, \end{aligned}$$

where $\mathbf{W}'_1 \in \mathbb{R}^{256 \times d_h}$, $\mathbf{W}'_2 \in \mathbb{R}^{128 \times 256}$, $\mathbf{W}'_3 \in \mathbb{R}^{1 \times 128}$ are learnable weights, and $s \in \mathbb{R}$ is the predicted grasp quality score. The detailed architecture of the proposed network is illustrated in Figure 1.

D. Dataset Generation

A training dataset which accurately reflects feasible grasp configurations is essential for effective model performance. The data used in developing and evaluating GtG 2.0 is from the GraspNet-1Billion [27] benchmark, which includes 100 training scenes, as well as 90 test scenes that each were captured by 256 different camera poses. Although GraspNet-1Billion provides large-scale annotations, it sometimes labels physically infeasible grasps as valid. Figure 3 illustrates discrepancies between GraspNet-1Billion’s original scores and recalculated quality scores, revealing that many grasps labeled as *valid* are actually collision-prone. To address this issue, GPG is used to generate new grasp candidates aligned with the parallel-jaw geometry. Each candidate is rescored using the GraspNet-1Billion evaluator to ensure consistency with the gripper’s constraints. This approach also aligns the training data with the distribution of grasps encountered during inference, avoiding out-of-distribution poses. Figure 4 summarizes the data quality distribution.

TABLE III
RESULTS OF ALL METHODS ON THE GRASPNET-1BILLION (APS ON REALSENSE/KINECT SPLIT).
COLOR-CODE RANKING: **RED**=1ST, **GREEN**=2ND, **BLUE**=3RD.

Method	Seen	Similar	Novel	Average
GPD [4]	22.87 / 24.38	21.33 / 23.18	8.24 / 9.58	17.48 / 19.05
PointnetGPD [9]	25.96 / 27.59	22.68 / 24.38	9.23 / 10.66	19.29 / 20.88
RGB Matters [11]	27.98 / 32.08	27.23 / 30.40	12.25 / 13.08	22.49 / 25.19
REGNet [12]	37.00 / 37.76	27.73 / 28.69	10.35 / 10.86	25.03 / 25.77
TransGrasp [29]	39.81 / 35.97	29.32 / 29.71	13.83 / 11.41	27.65 / 25.70
GraNet [21]	43.33 / 41.48	39.98 / 35.29	14.90 / 11.57	32.73 / 29.44
Zhuang, C. <i>et al.</i> [23]	50.12 / 45.30	43.90 / 40.00	16.94 / 13.33	36.99 / 32.88
GSNet [13]	67.12 / 63.50	54.81 / 49.18	24.31 / 19.78	48.75 / 44.15
Scale Balanced Grasp [30]	63.83 / -	58.46 / -	24.63 / -	48.97 / -
HGGD [14]	59.36 / 60.26	51.20 / 48.59	22.17 / 18.43	44.24 / 42.43
FlexLoG [18]	72.81 / 69.44	65.21 / 59.01	30.04 / 23.67	56.02 / 50.67
RNGNet [19]	76.28 / 72.89	68.26 / 59.42	32.84 / 26.12	59.13 / 52.81
GtG2.0 (Ours)	68.79 / 62.61	61.71 / 53.93	29.75 / 24.45	53.42 / 47.00

TABLE IV
ABLATION STUDIES ON DIFFERENT COMPONENTS. RESULTS OBTAINED FROM A FIXED SUBSET OF ANNOTATION IDS RANGING FROM 0 TO 255 IN INCREMENTS OF 10, FOR THE REALSENSE SPLIT.

Configuration	Average (APs(%))
Inside Points Only	45.29
Inside & Outside Points	48.57
Ensemble of 5 Models	53.69

E. Implementation and Training Process

As illustrated in Figure 4, collision and low-quality grasps dominate the dataset, resulting in severe class imbalance. This imbalance poses significant challenges for training generalizable models. To address this issue, an ensemble training strategy is implemented, consisting of five models sharing the same architecture described in Section III-C, each initialized with different weights and trained on using different train and val partitions. The models were developed using PyG [28], with the Mean Squared Error (MSE) loss function and a learning rate of 0.01. For each model, data corresponding to annotation ID = 0 was used, with 90% of the training scenes serving as the training set and the remaining 10% designated for validation. Additionally, to further alleviate class imbalance, a dynamic data-sampling approach is adopted. Specifically, every 10 epochs, the training set is refreshed and includes all feasible (high-quality) grasps, along with 50,000 randomly selected collision grasps and 50,000 randomly selected low-quality grasps. Each individual model was trained for 500 epochs, and during inference, predictions from the ensemble are averaged to yield the final grasp quality score.

IV. EXPERIMENTS

In this section, a comprehensive evaluation of GtG 2.0 is provided, incorporating both large-scale benchmarks and real-world robot experiments. The following subsections present results on the GraspNet-1Billion dataset to compare GtG 2.0 with a variety of state-of-the-art methods. Subsequently, ablation studies are described to examine the impact of key architectural components. Finally, the performance of GtG 2.0

is demonstrated on a 3-Dof Delta Parallel robot, highlighting the framework’s applicability under real-world conditions.

A. GraspNet-1Billion Benchmark Evaluation

The performance of GtG 2.0 was first assessed using the GraspNet-1Billion dataset and its official API. In this benchmark, AP serves as the primary evaluation metric. Each predicted grasp pose is validated over a range of fraction coefficients μ (from 0.2 to 1.0, in increments of 0.2), and the final AP is computed by averaging the resulting Precision@k values across all μ values [31]. A visualization of the final 50 grasps evaluated by the GraspNet benchmark is illustrated in Fig 5.

1) *Comparative Evaluation of Hypothesis-and-Test Methods*: The GraspNet-1Billion Benchmark Evaluation demonstrates that the proposed GTG 2.0 outperforms established Hypothesis-and-Test approaches, GPD and PointnetGPD, as shown in Table I. GTG 2.0 achieves higher AP across all of the parts of the test split while requiring significantly fewer parameters (0.57M compared to 3.6M and 1.6M, respectively), and this clearly demonstrated the effectiveness of GtG 2.0 as a new Hypothesis-and-Test method.

2) *Comparative Evaluation with Other GNN-based Methods*: As shown in Table II, GTG2.0 achieves significantly better performance compared to GraNet and the parallel graph network introduced in [23]. This improvement highlights the effectiveness of utilizing information about the surrounding areas of the grasp, in contrast to other methods, which rely on scene-level information. By capturing more balanced spatial details about the grasp area and its surroundings, GTG2.0 is able to make more accurate predictions, resulting in higher performance across all evaluation metrics.

3) *Comparative Evaluation of all Grasp Detection Methods*: Table III indicates that GTG2.0 ranks among the top three when compared to end-to-end models. This highlights the effectiveness of GNNs in detecting grasp poses within cluttered scenes. Notably, GTG2.0 achieved excellent performance by utilizing GNNs and considering the volume both inside and outside the gripper, while also benefiting from the flexibility exhibited by Hypothesis-and-Test methods.

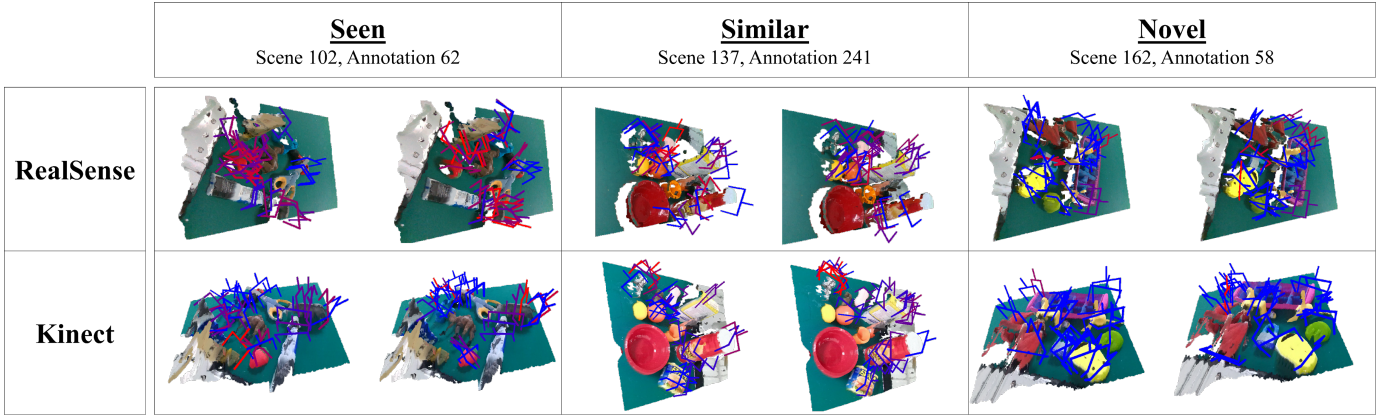


Fig. 5. Visualization of the final 50 grasps evaluated by the GraspNet benchmark. Each subimage shows 25 top-scoring grasps overlaid on the scene from different viewpoints. Warmer colors (reds and oranges) indicate higher predicted grasp success scores, while cooler colors (blues and purples) represent lower-scoring grasps. Grouping the grasps into two sets of 25 each makes it easier to see details on the objects, as opposed to plotting all 50 at once.

TABLE V

RESULTS OF THE 4-DOF ROBOT GRASPING EXPERIMENTS CONDUCTED USING A 3-DOF DELTA PARALLEL ROBOT EQUIPPED WITH A TWO-FINGER GRIPPER AND A KINECT-V1 SENSOR IN CLUTTERED SCENARIOS, REPORTING FOR EACH SCENE THE NUMBER OF OBJECTS PRESENT, THE NUMBER OF SUCCESSFUL GRASPS ACHIEVED, AND THE TOTAL NUMBER OF GRASP ATTEMPTS.

Scene	#Objects	Success	Attempts
1	5	5	5
2	5	5	6
3	6	6	7
4	8	8	8
5	6	6	7
Success Rate		30 / 33 = 91%	
Completion Rate		5 / 5 = 100%	

4) *Ablation Studies*: Ablation studies were conducted to assess the contributions of different components in GtG 2.0. A fixed subset of annotation IDs—ranging from 0 to 255 in increments of 10—was selected from the RealSense Split for this purpose. In Table IV, the results for three configurations are reported: First, when only the inside points are used (as in GPD and PointNetGPD), Second, when both inside and outside points are incorporated to provide richer contextual information, and third when the ensemble strategy, as outlined in Section III-E, is employed. It was observed that the inclusion of external points resulted in an improvement of the average AP from 45.29% to 48.57%, indicating that richer contextual information allows the graspable regions to be delineated more accurately. Furthermore, the performance was boosted to 53.69% by employing the ensemble strategy, which suggests that individual model errors are mitigated by averaging predictions from multiple independently trained models, thereby resulting in a more robust grasp prediction framework.

B. Real-World Testing with a 3-Dof Delta Parallel Robot

Although the GraspNet-1Billion benchmark provides a thorough simulation-based assessment, real-world validation remains essential. GtG 2.0 was therefore evaluated on a 3-Dof

Delta Parallel robot equipped with a two-finger gripper [32], which was built at the Human and Robot Interaction Laboratory, University of Tehran, and is inspired by the gripper made by robotiq [33]. The overall setup is illustrated in Figure 6(a). A Kinect v1 camera and a custom 3-Dof grasp candidate generator were utilized, because the original 7-Dof generator is not directly compatible with a 4-Dof system. The procedure followed for real-world testing is described below:

- 1) **Test Objects and Scene Setup**: A set of nine household objects, each with distinct shapes and materials, was chosen. In every trial, 5 to 8 objects were arranged randomly within the robot’s workspace to form cluttered scenarios (Figure 6(b)).
- 2) **Point Cloud Acquisition and Processing**: A Kinect v1 camera captured raw point clouds, which were transformed into the global robot frame. A weighted k -nearest neighbors filter ($k = 10$) was applied to reduce noise, followed by 2 mm voxel downsampling to preserve essential geometry.
- 3) **Heuristic 4-Dof Candidate Generation**: The grasp space was discretized by subdividing (x, y, z) coordinates in 1 cm intervals. Each point was replicated at successively lower z -values to fill potential gaps. Rotation around the z -axis was discretized in 30-degree increments, and a uniform 10 cm gripper width was assigned to each candidate.
- 4) **Grasp Scoring and Execution**: Graph representations were constructed for each candidate and evaluated by the trained GNN ensemble. The highest-scoring grasp pose was then executed by the robot.

By following the above steps, which are illustrated in Figure 6(c), an overall success rate of 91% was attained across five distinct test scenes, each containing 5–8 objects. Every scene was cleared successfully, yielding a completion rate of 100%. These results, summarized in Table V, highlight the adaptability and robustness of GtG 2.0, even under different sensor configurations and a generator with different constraints.

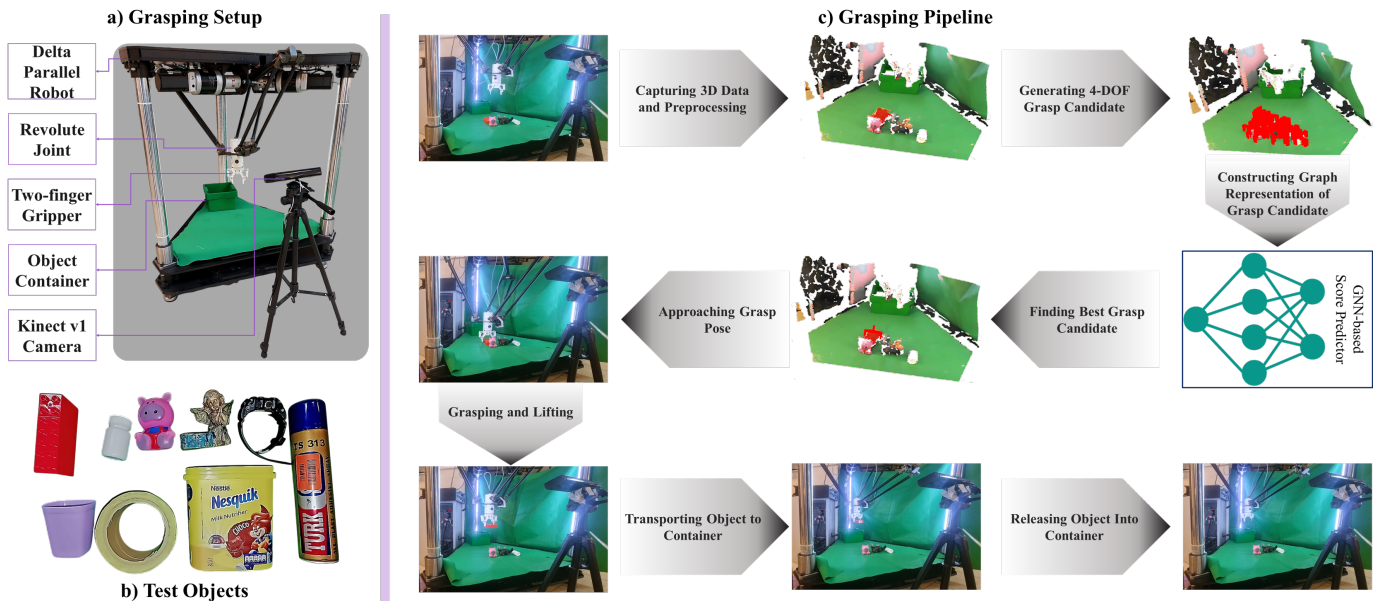


Fig. 6. (a) Experimental setup featuring a 3-DOF Delta Parallel robot, a two-finger gripper, and a Kinect v1 sensor, used to evaluate grasping performance in cluttered scenes. (b) Nine everyday objects used for real-world experiments, featuring diverse shapes, sizes, and materials. (c) The robot performs the full grasping task, including data acquisition, candidate generation, and object manipulation, as illustrated by the flow of actions from capturing 3D data to releasing the object into a container.

V. CONCLUSION

In this work, GtG 2.0—a novel Hypothesis-and-Test framework for high-precision grasp pose detection in cluttered scenes—was introduced, with an ensemble of lightweight GNNs being leveraged. The inherent flexibility of Hypothesis-and-Test methods is preserved by the approach, and the number of parameters is significantly reduced—by up to six times compared to conventional methods—while improvements of up to 35% in AP on the GraspNet-1Billion benchmark were achieved. Furthermore, when compared with recent end-to-end GNN-based methods, superior performance was consistently demonstrated by GtG 2.0, with the effectiveness of incorporating both inside and outside point representations for enriched geometric context being highlighted instead of the use of scene-level information. Despite these promising results, several limitations are still present. First, although a diverse set of candidates is efficiently produced by GPG, further improvements in the development of a more sophisticated generator which yields an even higher percentage of quality grasps are possible, likely through the use of improved heuristics. Additionally, although GtG 2.0 is ranked among the top-performing methods, a broader challenge common to all current approaches is highlighted by the presented results: the absolute performance on novel scene splits is maintained at a lower level than that on the Seen and Similar splits. An opportunity for further research aimed at enhancing the generalization capabilities of grasp detection frameworks across diverse and unseen environments is indicated by this general limitation.

REFERENCES

- [1] S. Khoshraftar and A. An, “A survey on graph representation learning methods,” *ACM Transactions on Intelligent Systems and Technology*, vol. 15, no. 1, pp. 1–55, 2024.
- [2] P. Veličković, “Everything is connected: graph neural networks,” *Current Opinion in Structural Biology*, vol. 79, p. 102538, 2023.
- [3] A. R. Moghadam, M. T. Masouleh, and A. Kalhor, “Grasp the graph (gtg): A super light graph-rl framework for robotic grasping,” in *2023 11th RSI International Conference on Robotics and Mechatronics (ICRoM)*, 2023, pp. 861–868.
- [4] M. Gualtieri, A. ten Pas, K. Saenko, and R. Platt, “High precision grasp pose detection in dense clutter,” in *2016 IEEE/RSJ International Conference on Intelligent Robots and Systems (IROS)*, Oct. 2016, pp. 598–605, iSSN: 2153-0866. [Online]. Available: <https://ieeexplore.ieee.org/document/7759114>
- [5] R. Platt, “Grasp learning: Models, methods, and performance,” vol. 6, no. 1, pp. 363–389. [Online]. Available: <https://www.annualreviews.org/doi/10.1146/annurev-control-062122-025215>
- [6] J. Mahler, J. Liang, S. Niyaz, M. Laskey, R. Doan, X. Liu, J. A. Ojea, and K. Goldberg, “Dex-net 2.0: Deep learning to plan robust grasps with synthetic point clouds and analytic grasp metrics,” in *Robotics: Science and Systems XIII, Massachusetts Institute of Technology, Cambridge, Massachusetts, USA, July 12-16, 2017*, N. M. Amato, S. S. Srinivasa, N. Ayanian, and S. Kuindersma, Eds., 2017. [Online]. Available: <http://www.roboticsproceedings.org/rss13/p58.html>
- [7] A. Ten Pas, M. Gualtieri, K. Saenko, and R. Platt, “Grasp pose detection in point clouds,” *The International Journal of Robotics Research*, vol. 36, no. 13-14, pp. 1455–1473, 2017.
- [8] R. Q. Charles, H. Su, M. Kaichun, and L. J. Guibas, “PointNet: Deep learning on point sets for 3d classification and segmentation,” in *2017 IEEE Conference on Computer Vision and Pattern Recognition (CVPR)*, pp. 77–85, ISSN: 1063-6919. [Online]. Available: <https://ieeexplore.ieee.org/document/8099499>
- [9] H. Liang, X. Ma, S. Li, M. Görner, S. Tang, B. Fang, F. Sun, and J. Zhang, “PointNetGPD: Detecting Grasp Configurations from Point Sets,” in *2019 International Conference on Robotics and Automation (ICRA)*, May 2019, pp. 3629–3635, arXiv:1809.06267 [cs]. [Online]. Available: <http://arxiv.org/abs/1809.06267>
- [10] S. S. Mohammadi, N. F. Duarte, D. Dimou, Y. Wang, M. Taiana, P. Morerio, A. Dehban, P. Moreno, A. Bernardino, A. Del Bue *et al.*, “3dsgrasp: 3d shape-completion for robotic grasp,” in *2023 IEEE international conference on robotics and automation (ICRA)*. IEEE, 2023, pp. 3815–3822.
- [11] M. Gou, H.-S. Fang, Z. Zhu, S. Xu, C. Wang, and C. Lu, “Rgb matters: Learning 7-dof grasp poses on monocular rgbd images,” in *2021 IEEE*

- International Conference on Robotics and Automation (ICRA)*. IEEE, 2021, pp. 13 459–13 466.
- [12] B. Zhao, H. Zhang, X. Lan, H. Wang, Z. Tian, and N. Zheng, “Regnet: Region-based grasp network for end-to-end grasp detection in point clouds,” in *2021 IEEE international conference on robotics and automation (ICRA)*. IEEE, 2021, pp. 13 474–13 480.
- [13] C. Wang, H.-S. Fang, M. Gou, H. Fang, J. Gao, and C. Lu, “Graspnet discovery in clutters for fast and accurate grasp detection,” in *Proceedings of the IEEE/CVF International Conference on Computer Vision*, 2021, pp. 15 964–15 973.
- [14] S. Chen, W. Tang, P. Xie, W. Yang, and G. Wang, “Efficient Heatmap-Guided 6-Dof Grasp Detection in Cluttered Scenes,” *IEEE Robotics and Automation Letters*, vol. 8, no. 8, pp. 4895–4902, Aug. 2023. [Online]. Available: <https://ieeexplore.ieee.org/document/10168242>
- [15] H. Liu, H. Li, C. Jiang, S. Xue, Y. Zhao, X. Huang, and Z. Jiang, “Structured local feature-conditioned 6-dof variational grasp detection network in cluttered scenes,” *IEEE/ASME Transactions on Mechatronics*, 2024.
- [16] S. Yu, D.-H. Zhai, and Y. Xia, “Robotic grasp detection based on category-level object pose estimation with self-supervised learning,” *IEEE/ASME Transactions on Mechatronics*, vol. 29, no. 1, pp. 625–635, 2023.
- [17] H. Hosseini, M. Koosheshi, M. T. Masouleh, and A. Kalhor, “Multi-modal robust geometry primitive shape scene abstraction for grasp detection,” *IEEE Access*, 2024.
- [18] W. Tang, S. Chen, P. Xie, D. Hu, W. Yang, and G. Wang, “Rethinking 6-dof grasp detection: A flexible framework for high-quality grasping,” *CoRR*, vol. abs/2403.15054, 2024. [Online]. Available: <https://doi.org/10.48550/arXiv.2403.15054>
- [19] S. Chen, P. Xie, W. Tang, D. Hu, Y. Dai, and G. Wang, “Region-aware grasp framework with normalized grasp space for efficient 6-dof grasping,” in *8th Annual Conference on Robot Learning*, 2024. [Online]. Available: <https://openreview.net/forum?id=jPkOFAiOzf>
- [20] X. Lou, Y. Yang, and C. Choi, “Learning object relations with graph neural networks for target-driven grasping in dense clutter,” in *2022 International Conference on Robotics and Automation (ICRA)*, 2022, pp. 742–748.
- [21] H. Wang, W. Niu, and C. Zhuang, “Granet: A multi-level graph network for 6-dof grasp pose generation in cluttered scenes,” in *2023 IEEE/RSJ International Conference on Intelligent Robots and Systems (IROS)*, 2023, pp. 937–943.
- [22] Z. Hu, Y. Zheng, and J. Pan, “Living object grasping using two-stage graph reinforcement learning,” *IEEE Robotics and Automation Letters*, vol. 6, no. 2, pp. 1950–1957, 2021.
- [23] C. Zhuang, H. Wang, W. Niu, and H. Ding, “A parallel graph network for generating 7-dof model-free grasps in unstructured scenes using point cloud,” *Robotics and Computer-Integrated Manufacturing*, vol. 92, p. 102879, 2025. [Online]. Available: <https://www.sciencedirect.com/science/article/pii/S0736584524001662>
- [24] Y. Eldar, M. Lindenbaum, M. Porat, and Y. Zeevi, “The farthest point strategy for progressive image sampling,” in *Proceedings of the 12th IAPR International Conference on Pattern Recognition*, 1994, pp. 93–97 vol.3.
- [25] H. Liang, “Python binding for grasp pose generator (pygpg),” Aug. 2021. [Online]. Available: <https://doi.org/10.5281/zenodo.5247189>
- [26] W. Hamilton, Z. Ying, and J. Leskovec, “Inductive representation learning on large graphs,” *Advances in neural information processing systems*, vol. 30, 2017.
- [27] H.-S. Fang, C. Wang, M. Gou, and C. Lu, “Graspnet-1billion: A large-scale benchmark for general object grasping,” in *Proceedings of the IEEE/CVF conference on computer vision and pattern recognition*, 2020, pp. 11 444–11 453.
- [28] M. Fey and J. E. Lenssen, “Fast graph representation learning with pytorch geometric,” *arXiv preprint arXiv:1903.02428*, 2019.
- [29] Z. Liu, Z. Chen, S. Xie, and W. Zheng, “Transgrasp: A multi-scale hierarchical point transformer for 7-dof grasp detection,” in *2022 International Conference on Robotics and Automation (ICRA)*. IEEE Press, 2022, p. 1533–1539. [Online]. Available: <https://doi.org/10.1109/ICRA46639.2022.9812001>
- [30] H. Ma and D. Huang, “Towards scale balanced 6-dof grasp detection in cluttered scenes,” *CoRR*, vol. abs/2212.05275, 2022. [Online]. Available: <https://doi.org/10.48550/arXiv.2212.05275>
- [31] T.-Y. Lin, M. Maire, S. Belongie, J. Hays, P. Perona, D. Ramanan, P. Dollár, and C. L. Zitnick, “Microsoft coco: Common objects in context,” in *Computer Vision—ECCV 2014: 13th European Conference, Zurich, Switzerland, September 6–12, 2014, Proceedings, Part V 13*. Springer, 2014, pp. 740–755.
- [32] P. Yarmohammadi, N. A. Khomami, M. T. Masouleh, and M. R. Zakerzadeh, “Experimental study on chess board setup using delta parallel robot based on deep learning,” in *2023 11th RSI International Conference on Robotics and Mechatronics (ICRoM)*. IEEE, 2023, pp. 869–875.
- [33] L.-A. A. Demers, S. Lefrançois, and J.-P. Jobin, “Gripper having a two degree of freedom underactuated mechanical finger for encompassing and pinch grasping,” Mar. 10 2015, uS Patent 8,973,958.